RESEARCH ARTICLE

Application of decoy oligodeoxynucleotides strategy for inhibition of cell growth and reduction of metastatic properties in nonresistant and erlotinib-resistant SW480 cell line

Zoleykha Asadi[1] | Mojtaba Fathi[2,3] | Elham Rismani[4] | Zahra Bigdelou[1] | Behrooz Johari[3,5] (ID)

[1]Department of Medical Biotechnology, School of Medicine, Zanjan University of Medical Sciences, Zanjan, Iran

[2]Department of Clinical Biochemistry, School of Medicine, Zanjan University of Medical Sciences, Zanjan, Iran

[3]Cancer Gene Therapy Research Center, Zanjan University of Medical Sciences, Zanjan, Iran

[4]Molecular Medicine Department, Pasteur Institute of Iran, Tehran, Iran

[5]Zanjan Pharmaceutical Biotechnology Research Center, Zanjan University of Medical Sciences, Zanjan, Iran

Correspondence
Mojtaba Fathi, Department of Clinical Biochemistry, School of Medicine, Zanjan University of Medical Sciences, Zanjan, Iran.
Email: m_fathi@zums.ac.ir

Behrooz Johari, Department of Medical Biotechnology, School of Medicine, Zanjan University of Medical Sciences, Zanjan, Iran.
Email: Dr.Johari@zums.ac.ir

Funding information
Zanjan University of Medical Sciences, Grant/Award Number: A-12-802-24

Abstract

Signal transducer and activator of transcription 3 (STAT3) is a critical regulator for angiogenesis, cell cycle progression, apoptosis, and drug resistance. Resistance toward EGF receptor (EGFR) inhibitors is a significant clinical concern for metastatic colon cancer patients. The present study aimed to evaluate the blocking influences of STAT3 decoy oligodeoxynucleotides (ODNs) on the STAT3 survival signaling pathway in nonresistant and erlotinib-resistant SW480 colon cancer cells. First, STAT3 decoy and scramble ODNs were designed according to STAT3 elements in the promoter region of MYCT1 gene and tested for the interaction of STAT3 protein with designed ODNs via in silico molecular docking study. Then, the efficiency of transfection and subcellular localization of ODNs were assessed using flow cytometry and fluorescence microscopy, respectively. Cell viability, cell cycle, and apoptosis tests, scratch and colony formation assays, and real-time PCR were also used to study the cancerous properties of cells. A considerable decrease in proliferation of colon cancer cells was observed with blockade of STAT3 signaling due to cell cycle arrest and induced apoptosis via downregulation of cyclin D1 and Bcl-XL, respectively. Furthermore, upon transfecting STAT3 decoy ODNs, colony formation potential and migration activity in both SW480 colon cancer cell lines were decreased compared to the control groups. From this study, it could be concluded that STAT3 is critical for cell growth inhibition and metastatic properties reduction of resistant SW480 colon cancer cells; therefore, STAT3 decoy ODNs could be considered as potential therapeutics along with current remedies for treating drug-resistant colon cancer.

KEYWORDS
colon cancer, decoy oligodeoxynucleotides, drug resistance, erlotinib, STAT3 transcription factor

1 | INTRODUCTION

Colorectal cancer (CRC), as a paramount public health burden, is responsible for almost 1.2 million new cases of cancer each year (Troiani et al., 2014). In the past 30 years, surgery, radiotherapy, chemotherapy, and combinations of them have been considered as the major treatments for various cancers. New therapeutic approaches including targeted drug delivery, thermotherapy, gene therapy, and immunotherapy have raised the variety of treatment options and enabled personalized medicines, but the desired outcome has not yet been achieved for cancer patients. One substantial cause for ineffectiveness of therapies is the intrinsically possessed or gradually developed resistance of the cancer cells. Drug resistance in cancer therapy is a multifactorial phenomenon that could be the consequence of drug intracellular distribution, structural alteration of its molecular target, apoptosis inhibition, or increased activity of some enzymes (Szakács et al., 2006; Hajighasemlou et al., 2015).

Earlier reports have indicated that STAT3 could be a potential predictive signaling factor that is involved in CRC oncogenesis and epidermal growth factor receptor (EGFR) signaling pathway (Dobi et al., 2013; Li et al., 2013). Preclinical studies have shown the synergistic effect of Cetuximab and erlotinib co-treatment on growth inhibition of colon cancer cells, both as an outcome of promoted suppression of the EGFR pathway and differential influences on STAT3. Although, erlotinib inhibits effectively the EGFR, the progress of resistance to erlotinib during chemotherapy has led to treatment failure (Gharibi et al., 2020; Javadi et al., 2018; Weickhardt et al., 2012). These days, the combination of several therapeutic medications has become the main strategy for combating drug-resistant cancers including RNAi (Chen et al., 2009; Roberts et al., 2017), antisense oligonucleotides (Preston et al., 2003), aptamers, ribozymes (Snir et al., 2003), and decoy oligodeoxynucleotides (Johari et al., 2019; Lasala & Minguell, 2011).

Targeting the transcription factors is an alternative option to intervene in an activated regulatory pathway that stimulates metastasis. Transcription factor decoy (TFD) oligodeoxynucleotides (ODNs) is classified as a new group of nucleic acid-based treatment, which are short double-stranded DNA molecules (Hu & Zhang, 2012). STAT3 is a master regulator transcription factor for Bcl-2 and Bcl-XL gene expression. Erlotinib-mediated activation of STAT3 has been reported to up-regulate Bcl-2/Bcl-XL, resulting in resistance of cancer cells toward regular therapies. Considering the role of STAT3 as a key mediator in a vast range of malignancies, it could be an appropriate target for cancer therapy approaches (Gu et al., 2008; Sen et al., 2012a; Tong et al., 2017).

Previous reports revealed that the mechanism of designed hairpin STAT3-decoy ODNs is based on a serum-inducible element of the human c-fos promoter in SW480 colon carcinoma cells (Souissi et al., 2011; Tadlaoui Hbibi et al., 2009). In our previous study on erlotinib-resistant colon cancer cells, it was indicated that cellular metabolism changes in resistant colon cancer cells (Javadi et al., 2018). In the current study, it was aimed to inhibit the STAT3 signaling pathway by using decoy ODNs strategy to investigate the anticancer influences of this strategy on both nonresistant and erlotinib-resistant SW480 colon cancer cell lines.

2 | MATERIALS AND METHODS

2.1 | In silico molecular docking analysis

In silico methods have been shown to provide valuable information regarding various molecular interactions in biological studies (Haghighi & Moradi, 2020; Nabati et al., 2020). In this study, three-dimensional models of designed ODNs (decoy and scramble) were constructed by 3D-DART tool (Bigdelou et al., 2019). The designed B-DNA conformation of sequences were compatible with the structural analysis of DNA in a complex with proteins (van Dijk & Bonvin, 2009). The crystal structure of STAT3 protein was provided from RCSB Protein Data Bank (PDB ID: 1BG1). The molecular interactions of STAT3 protein and ODNs (decoy and scrambled) were evaluated by molecular docking approach, using HADDOCK webserver (van Zundert et al., 2016; Wassenaar et al., 2012). The predicted nucleic acid-protein complexes were analyzed using Ligplot + program (Laskowski & Swindells, 2011). PyMOL program was used to visualize the results of the docking complex.

2.2 | ODNs synthesis for STAT3 transcription factor

The design of STAT3 decoy oligodeoxynucleotides was based on the STAT3 elements in the promoter region of the human MYCT1 gene (Triner et al., 2018). The sequence of the scramble (SCR) was obtained by three mutations in nucleotides of the core binding site. The core region which is demonstrated in bold, and mutations in SCR are designated in italics/underlined. The ODNs were labeled at the 3′ terminus with Cy3 fluorescent dye for tracking the localizations (Bioneer, Korea). Cy3-labeled ODNs were prepared by dissolving in sterile TE buffer (10 mM Tris, 1 mM EDTA, pH 8.0). The stability of sequences was improved by phosphorothioate (PS) modification at 3' and 5' (presented by asterisk). Preparation of lyophilized ODNs was conducted as described in an earlier report (Rahmati et al., 2020). In brief, ODNs were diluted in TE buffer (10 mmol/L Tris–HCl, 0.1 mmol/L EDTA, 0.1 mol/L NaCl, pH (8.0), annealed at 95°C for 10 min and cooled gradually to reach the room temperature. The ODNs quantities were determined by NanoDrop™ spectrophotometry. The sequences of designed ODNs are as the following:

Decoy ODNs
[5′-G*TGCAC**TTTCCTGAA**TTTTT*A-3′]
[3′-CACGTGAAAGGACTTAAAAAT-5′]
SCR ODNs:
[5′-G*TGCACTTT*G*CT*C*G*ATTTTTA*-3′]
[3′-CACGTGAAACGAGCTAAAAAT-5′]

2.3 | Cell culture

The SW480 colon cancer cell line was obtained from Pasture Institute of Iran (ATCC: CCL-228), cultivated in RPMI 1640 medium (Gibco), complemented with 1% penicillin–streptomycin (Gibco), and 10% fetal bovine serum (Gibco) and incubated in 5% CO_2 at 37°C.

2.4 | Establishing erlotinib-resistant SW480 cell line

Induction of resistance in erlotinib-sensitive SW480 cells was carried out as earlier reported with some minor modifications (Javadi et al., 2018). In brief, cells were exposed to 20 μM erlotinib for three days, followed by 5 days' recovery, then sequential treatment/recovery for a total of four cycles. The resistant cell line was cultured with the maximum concentration of erlotinib to allow cellular proliferation. Thereafter, the mean inhibitory concentration (IC_{50}) of erlotinib was investigated for resistant and nonresistant cells.

2.5 | Decoy ODNs transfection efficiency analysis

Erlotinib-resistant SW480 cells (5×10^4 cells/well) were seeded in 24-well plates. At the confluency of 60%–70%, the media was exchanged with Opti-RPMI (Gibco) containing Cy3-labeled ODN-Lipofectamine 2000 complexes (100, 300, and 500 nM). Lipofectamine 2000 either was used alone as control or with elevating amounts of labeled ODNs in each transfection. Following 24 h of incubation at 37°C in a 5% CO_2 incubator, cells were detached using trypsin enzyme and washed with phosphate-buffered saline (PBS). The efficacy of transfection was determined based on Cy3-labeled ODNs via flow cytometry (BD Biosciences).

2.6 | Subcellular localization of transfected labeled ODNs

One day before transfection, the SW480 cells (5×10^4 cells/well) were cultivated in a 24-well plate for fluorescence microscopy investigation. Following the wash with PBS, cells were incubated with 500 nM Cy3-labeled decoy ODNs in the presence of 2 μl of Lipofectamine reagent/0.5 ml media per well for 24 h, at 37°C in 5% CO_2. Cells were fixed using 4% paraformaldehyde for 20 min. Afterward, they were treated with 1 μg/ml 4, 6-diamidino-2-phenylindole (DAPI) (Sigma) for 15 min and washed three times for 5 min in PBS. The nuclear DNA content of cells was visualized via fluorescence microscope equipped with Cy3 and DAPI filter sets (Olympus).

2.7 | Cell viability assay

Cell viability of both nonresistant and resistant SW480 cell lines was measured by 3-(4,5-dimethylthiazol-2-yl)-2,5-diphenyltetrazolium bromide (MTT) colorimetric assay in a time table of 24, 48, and 72 h. After 24 h of cell culture (8×10^3 cells/well) in 96-well plates, various concentrations (0, 10, 100, and 300 nM) of STAT3 decoy (as test group), scramble ODNs and Lipofectamine alone (as controls) were added to seeded cancer cell lines. At different times, the wells were treated with MTT solution (5 mg/ml, 15 μl/well) and incubated at 37°C for 4 h. Then, dimethylsulfoxide was added (150 μl/well) to each well, and the plates were agitated for 10 min. The optical absorbance was read at 570 nm by a Stat Fax-2100 microplate reader (Awareness Technology). Viability of cells was calculated as follows: (mean optical density [OD] of treated cells divided by mean OD of control cells) × 100.

2.8 | Cell cycle assay

Cell cycle assay was performed 24 and 72 h after transfecting by 300 nM of STAT3 decoy or scrambled ODNs, and Lipofectamine alone. The optimum cell density for transfection was 75×10^3 cells/12-well plate. Briefly, the washed cells with ice-cold saline were suspended in 100 μl of Dulbecco's phosphate-buffered saline (DPBS), and fixed with 900 μl of ethanol. The fixed cells were stored at –20°C for 20 min, pelleted, resuspended in 300 μl of staining buffer (1 mg/ml RNase, 20 μg/ml propidium iodine, 0.01% NP-40 in DPBS) and incubated at 37°C for 10 min. The DNA content of nuclei was analyzed via flow cytometry (BD Biosciences), using FlowJo software (Tree Star).

2.9 | Cell apoptosis assay

For apoptosis assay, a density of 75×10^3 cells/12-well plate was transfected with STAT3 decoy or scramble ODNs (300 nM) and Lipofectamine alone. After 24 and 72 h of transfection, detached cells were washed and resuspended in 100 μl annexin V binding buffer. Following, the cells were dyed with Annexin V-FITC and propidium iodide (Sigma), according to manufacturer's protocol. The cells were investigated via flow cytometry (BD Biosciences) and results were interpreted by FlowJo program (Tree Star).

2.10 | Soft agar colony-forming assay

The influence of STAT3 decoy on the colony-forming potency of non-resistant and erlotinib-resistant SW480 cells was evaluated through the modified suspension culture method (Liu et al., 2006). Briefly, the limited number of each cell line (100 cells per 200 μl) in nonadherent agar-coated 24-well plates (one plate for each cell line) were incubated in serum-free stem cell media (SCM; RPMI supplemented with B27; Life Technologies; 20 ng/ml EGF; Sigma; and 10 ng/ml fibroblast growth factor; Sigma) for 14 days to generate primary colonospheres. Following, the single-cell suspension was prepared by centrifuging (1000 rpm) the final colonospheres with 0.05% trypsin/EDTA. Thereafter, single-cells were cultured in nonadherent agar-coated 24-well plates in SCM and transfected with 300 nM of STAT3 decoy (test group), scrambled ODNs, and Lipofectamine alone as controls for each cell line. After the addition

of 500 µl culture media (RPMI 1640 medium with previously mentioned complements), the soft agar plates were incubated at 37°C in 5% CO_2 for 5 days. Every 48 h, each group was supplemented with 50 µl of transfection media. After 5 days, the size of generated colonospheres were investigated via light microscopy and image J program (1.52a; Phi et al., 2018).

2.11 | Scratch assay

The cell migration was assessed by the scratch assay. Nonresistant and Erlotinib-resistant SW480 cells (5×10^4 cells/ml) were cultivated in a 24-well plate for 24 h. Following the linear scratch using a 10 µl sterile pipette tip, the cells were exposed to STAT3 decoy and scramble ODNs treatments. After 48 h, wound healing was estimated through inverted light microscopy. The images were analyzed using Image J software (1.52a).

2.12 | Quantitative reverse-transcription polymerase chain reaction (qRT-PCR)

Quantitative expression of tumorigenesis markers (*Cycline D1/Bcl-XL*) was evaluated by real-time PCR. Total RNA was extracted from transfected cells using RNX–Plus reagent (Sinaclon). Following, it was reverse-transcribed with PrimeScript™ RT reagent Kit. Amplification was carried out by 2 × SYBR green PCR master mix (Amplicon) and specific primers (Rahmati et al., 2020) by ABI 7500 real-time PCR system (Applied Biosystems).

Relative gene expression was quantified by the $e^{-\Delta\Delta C_t}$ method, using GAPDH housekeeping gene as an internal control. Data were analyzed by Stepone software 2.3 v and represented as mean ± SD of three independent repeats.

2.13 | Statistical analysis

Statistical analysis was carried out by GraphPad Prism program version 6.0. The values are provided as mean ± SD. Experiments were carried out with a repetition of a minimum three times. One-/two-way analysis of variance (one/two ANOVA) was used as the statistical assay. Deviations were regarded as statistically meaningful at $^*p < .05$, $^{**}p < .01$, $^{***}p < .001$, and $^{****}p < .0001$.

3 | RESULT

3.1 | In silico docking analysis of protein and decoy ODNs

HADDOCK webserver provides a benchmark for modeling of the protein-DNA complex. Molecular docking of ODNs (decoy and scramble) with STAT3 protein resulted in generating STAT3-decoy and STAT3-scramble complex as well. The 2D representation of complex, using DIMPLOT program of Ligplot + software revealed the molecular contacts between amino acids and nucleotides. Results indicated particular interaction of STAT3 with the decoy and scramble ODNs molecules. Predominantly, a consensus binding site (5′-TTCCGGGAA-3′) is the target of STAT3 protein (Becker et al., 1998). Preserving this element in decoy ODNs resulted in higher interacting H-bonds between protein and decoy. Likewise, mutations in the binding site of the scramble ODNs with a nonspecific sequence (5′-TTTGCTCGA-3′) resulted in a smaller number of H-bonds in the scramble-STAT3 complex. The different number of H-bonds were nine and four H-bonds for decoy and scramble, respectively. It is demonstrating the higher compatibility of the complex structure of protein and decoy ODNs, rather than scramble. The STAT3 protein and scramble ODNs have three nonspecific interactions out of the binding site. The list of residues involved in H-bond interactions of ODNs and STAT3 has been summarized in Table 1. Finally, the models of STAT3 interactive configuration to decoy and scramble ODNs are depicted in Figure 1. The overall lowest-energy structure of STAT3-ODNs complexes showed the acceptable root-mean-square deviation (RMSD) of 0.6 and 0.7 for STAT3-decoy and STAT3-scramble complexes, respectively. The lower value of RMSD, the higher accordance of the complex model is in comparison to the overall structure. The energy profile of complexes indicated the stability of the folded state of complexes. Table 2 presents the interactive residue-nucleotides and docking energies of STAT3-ODNs.

3.2 | Establishing erlotinib-resistant SW480 colon cancer cell line

At the first 8 days of exposure to 20 µM erlotinib, the cell viability percentage of SW480 cells was considerably reduced, indicating the sensitivity of SW480 cells in the first time of treatment. Gradually in subsequent cycles of treatment, cells became resistant and cell
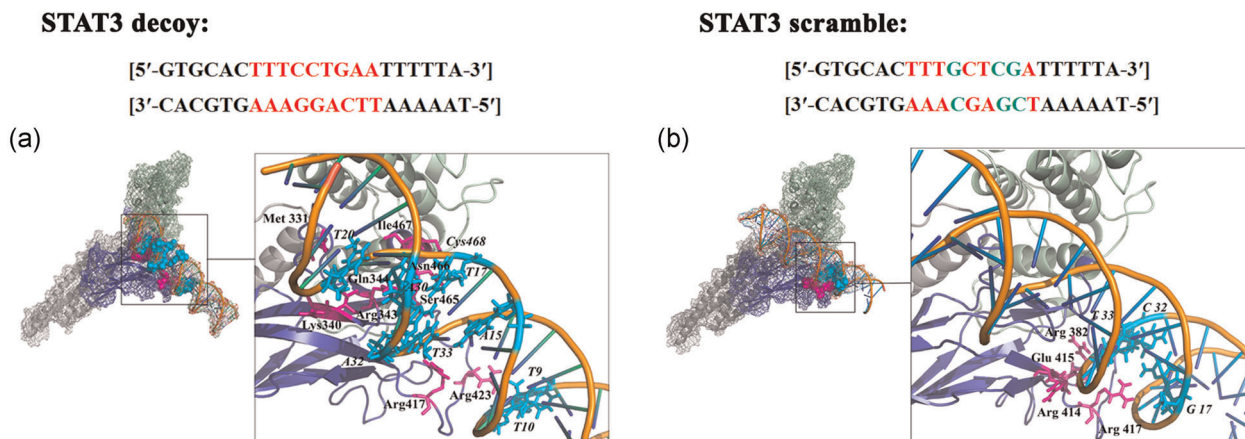
TABLE 1 Interactive residues and nucleotides in H-bonds of STAT3-ODNs

STAT3/decoy amino acids	Met331, Lys340, Gln344, Arg417, Arg423, Ser465, Asn466, Ile467, Cys468
STAT3/decoy nucleotides	T9, T10, A15, T17, T20, A30, A32, T33
STAT3/scramble amino acids	Arg382, Arg414, Glu415, Arg417
STAT3/scramble nucleotides	G17, C32, T33

Abbreviations: ODN, decoy oligodeoxynucleotide; STAT3, signal transducer and activator of transcription 3.

STAT3 decoy:

[5′-GTGCACTTTCCTGAATTTTTA-3′]

[3′-CACGTGAAAGGACTTAAAAAT-5′]

(a)

STAT3 scramble:

[5′-GTGCACTTTGCTCGATTTTTA-3′]

[3′-CACGTGAAACGAGCTAAAAAT-5′]

(b)

FIGURE 1 Complex structure of STAT3 protein and oligodeoxynucleotides. The STAT3 decoy ODNs (a) and the scramble ODNs (b), depicted in orange, were docked to DNA-binding site of STAT3 protein that is shown in blue. The binding site sequences of decoy and the mutated nucleotides of scramble are depicted in red and green, respectively. In the zoomed part of the images, the amino acids and nucleotides involved in the interactions of STAT3 and ODNs are shown in magenta and cyan, orderly. ODN, oligodeoxynucleotide; STAT3, signal transducer and activator of transcription 3

TABLE 2 Evaluation of interactive residue-nucleotides and docking energies of STAT3-ODNs

	STAT3/decoy	STAT3/scramble
Amino acids in H-bonds	Met331, Lys340, Gln344, Arg417, Arg423, Ser465, Asn466, Ile467, Cys468	Arg382, Arg414, Glu415, Arg417
Nucleotides in H-bonds	T9, T10, A15, T17, T20, A30, A32, T33	G17, C32, T33
HADDOCK score	−88.1 ± 2.6	−84.8 ± 6.7
RMSD from the overall lowest-energy structure	0.6 ± 0.3	0.7 ± 0.7
Van der Waals energy (kcal mol^{-1})	−53.0799 ± 2.8	−51.7413 ± 2.9
Electrostatic energy (kcal mol^{-1})	−447.036 ± 12.8	−405.222 ± 8.6
Desolvation energy (kcal mol^{-1})	−8.74 ± 4.2	−16.81 ± 2.8

Abbreviation: ODN, oligodeoxynucleotide; RMSD, root-mean-square deviation; STAT3, signal transducer and activator of transcription 3.

viability showed an increase (Figure 2a). The augment in the cell viability following the constant concentrations of erlotinib, together with the meaningful differences over time, indicated cell adaptation and induction of resistance.

The IC_{50} of erlotinib in nonresistant cells was 124/2 ± 1/2 nM, while it showed a dramatic increase to 19/86 ± 1/8 μM in the resistant cells (Figure 2b,c) which is another confirmation of resistance induced by erlotinib exposure.

3.3 | Transfection efficiency and intracellular localization of STAT3 decoy ODNs

According to the results of flow cytometry, the entrance of Cy3-labeled decoy ODNs into SW480 cells was dose-dependent. The calculated transfection efficiency indicated 90.5% at 500 nM and 90.48% at 300 nM of ODNs (Figure 3a,b). Regarding this fact, 300 nM ODNs was selected in the following experiments.

Fluorescence microscopy results indicated the subcellular localization of decoy ODNs (Figure 3c). The presence of fluorescent cells in micrographs displayed that cells were successfully transfected with Lipofectamine/Cy3-labeled STAT3 decoy ODNs. STAT3 decoy ODNs and nuclei counterstained with DAPI are presented in red and blue, orderly.

3.4 | STAT3 decoy ODNs reduce cell viability in nonresistant and resistant SW480 cells

Analysis of MTT assay for both nonresistant and resistant SW480 colon cancer cells treated with STAT3 decoy ODNs compared with the control group revealed a significant reduction of cell viability with a time- and dose-dependent pattern. Cell viability of nonresistant cells has declined more than resistant cells after treatment with 100 and 300 nM decoy ODN, where the effect was detected after 24 and 48 h of treatment in the nonresistant cells.
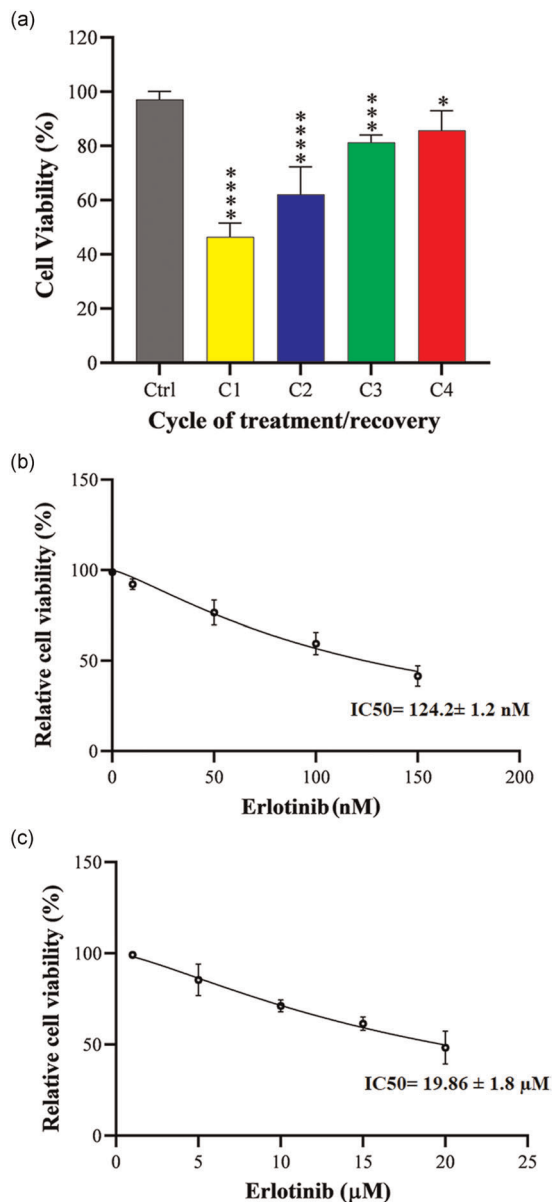
3.5 | STAT3 decoy ODNs induced cell-cycle arrest in nonresistant and resistant SW480 cells

Cell cycle profile of ODN-treated cells (nonresistant and resistant SW480 cells) was analyzed using flow cytometry assessment of DNA content by PI staining. The effects of the STAT3 decoy ODNs treatment on both cell lines were significant in cell cycle arrest, compared with the control groups. Whereas, the scramble ODN-treated cells showed no significant changes. After 24 h, the augment in the number of cells in the G0/G1 phase and the reduction in the number of cells in the S phase were detectable in the decoy-treated cell profile, and this effect was sustained for up to 72 h (Figure 5 and S1). Interestingly, in nonresistant SW480 treated with STAT3-ODNs, a considerable fraction of cells was in the G0/G1 phase, but there was a slight increase in erlotinib-resistant cells showing that proliferation inhibition in resistant cells was less affected by STAT3-ODNs than the nonresistant cells. Differences in cell cycle profiles of resistant and nonresistant SW480 cells were minimized after 72 h treatment with STAT3 decoy ODNs.

3.6 | STAT3 decoy ODNs induce apoptosis in nonresistant and resistant SW480 cells

Flow cytometry results revealed a remarkable enhancement in the apoptosis rate of nonresistant and resistant SW480 cells after 24 h treatment with STAT3-decoy ODNs compared with the control and scramble groups (Figure 6). Also, treatment with STAT3 decoy after 72 h caused less apoptotic cells in nonresistant and resistant SW480 cells (Figure S2). Following a 24 h STAT3 decoy transfection, the number of apoptotic cells was increased up to $17.23 \pm 5.59\%$ and $14.51 \pm 4.21\%$, in nonresistant and resistant cells, respectively. The results demonstrated a lower apoptotic influence of STAT3 decoy ODNs on resistant cancer cells, indicating the effect of increased STAT3 signaling on the cellular resistance.

3.7 | STAT3 decoy ODNs decreases colony formation in nonresistant and resistant SW480 cells

The colony formation potential of nonresistant and resistant SW480 cells was investigated in serum-free stem cell media for five days. The results indicated lower colony formation potential among STAT3 decoy ODNs-treated cells in comparison with the scrambled ODNs treated and control group cells (Figure 7a,b).

3.8 | STAT3 decoy ODNs reduce migration ability of nonresistant and resistant SW480 cells

Scratch assay was conducted to validate the migration potential of nonresistant and resistant-SW480 cells owing to ODNs treatments. Compared with the control and scramble-treated groups, migration
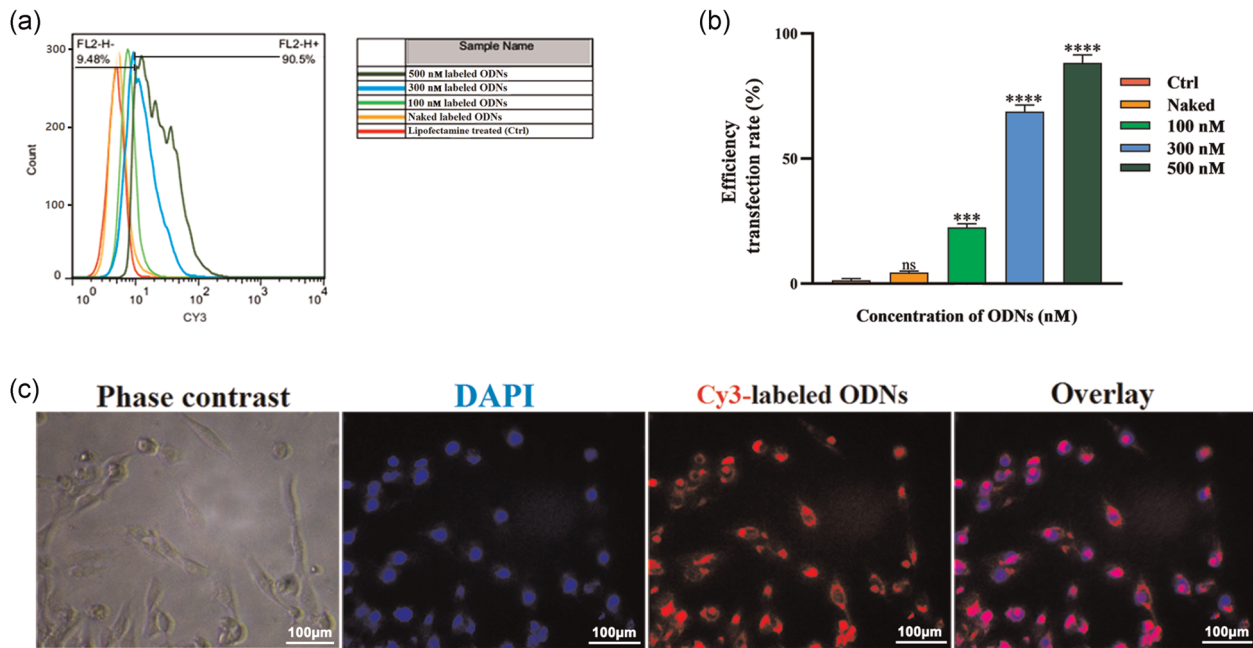
FIGURE 2 (a) The erlotinib effect on SW480 cell line. The cells were processed with 20 μM of erlotinib in four cycles of treat/recovery, and cell viability was analyzed using an MTT analysis. Values are reported as mean ± SD. The significant differences between treated cells at four cycle compared with those of control ones is designated as $*p < .05$, $***p < .001$, $****p < .0001$. Dose-dependent inhibitory influences of erlotinib on nonresistant and resistant SW480 colon cancer cells (b) cell viability of nonresistant SW480 colon cancer cells were determined after incubation with 0–150 nM erlotinib for 24 h. (c) Cell viability of resistant SW480 colon cancer cells were calculated after incubation with 0–20 μM erlotinib for 24 h. MTT, 3-(4,5-dimethylthiazol-2-yl)-2, 5-diphenyltetrazolium bromide

Altogether, the obtained results showed that decoy ODNs have a less inhibitory effect on cell viability of resistant cells than nonresistant cells, which may be due to the high activity of STAT3 transcription factor in these cells (Figure 4). In contrast, changes in the cell viability of scramble ODN-treated cells were negligible compared to the nontreated cells (control group).

FIGURE 3 Transfection of SW480 cells with STAT3 decoy ODNs. This assay was performed 24 h after treatment with Cy3-labeled decoy oligodeoxynucleotides. (a) Transfection efficiency of Cy3-labeled decoy ODNs detected via flow cytometry. (b) One-way ANOVA was used as the statistical analysis. The data are presented as mean ± SD of three independent experiments. Analyzing the efficiency of transfection was considered significant with ***$p < .001$, ****$p < .0001$ and ns, nonsignificant. (c) Fluorescent images of cells treated with Lipofectamine/Cy3-labeled STAT3 decoy ODNs 300 nM. STAT3 decoy ODNs and nuclei counterstained with DAPI are visible in red and blue, respectively. ANOVA, analysis of variance; DAPI, 4',6-diamidino-2-phenylindole; ODN, oligodeoxynucleotide; STAT3, signal transducer and activator of transcription 3
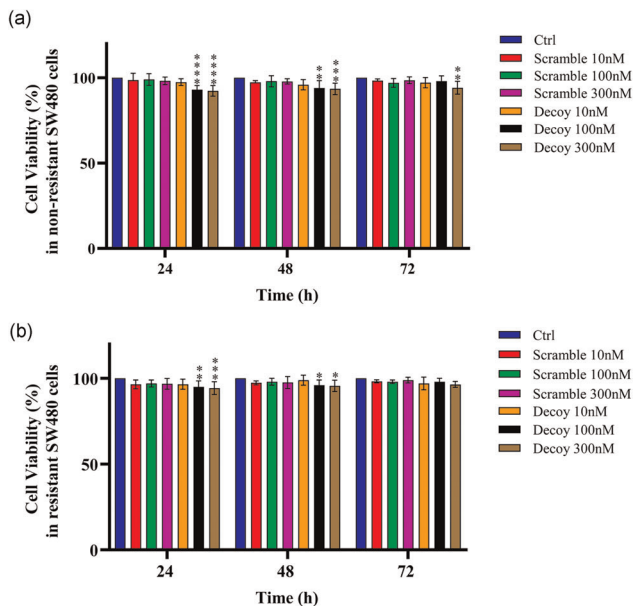

FIGURE 4 STAT3 decoy inhibited the cell viability in the cancer cells. After 24 h, (a) nonresistant and (b) resistant SW480 cells cultured in 96-well, were treated with STAT3 decoy and scramble ODNs along with Lipofectamine. Cell viability was assessed through MTT assay in three replicates per condition. Two-way ANOVA was used as the statistical analysis. The data are provided as mean ± SD of three independent experiments, *$p < .05$, **$p < .01$, ***$p < .001$, and ****$p < .0001$. ANOVA, analysis of variance; MTT, 3-(4,5-dimethylthiazol-2-yl)-2,5-diphenyltetrazolium bromide; ODN, oligodeoxynucleotide; STAT3, signal transducer and activator of transcription 3

and scratch filling in the decoy-treated group were significantly slower (Figure 8a,b).

The obtained results showed that decoy ODNs have approximately the same influence on cell migration in both nonresistant and resistant cells.

3.9 | STAT3 decoy ODNs alter the expression of target genes

Biological functions of STAT3 include regulating proliferation, apoptosis, and cell survival by mediating the regulation of antiapoptotic, oncogenic, and cell cycle genes. Relative gene expression analysis in the nonresistant and resistant SW480 treated cells revealed a notable decline in *Bcl-xl* and *cyclin D1*, as apoptosis marker and cell proliferation regulator, respectively. Alongside, there was a dramatic increase in STAT3 expression in cells after treatment with STAT3 ODNs decoy (Figure 9). RT-qPCR results confirmed the influence of STAT3 decoy ODNs transfection on stimulating apoptosis and cell cycle arrest in SW480 cells that could be related to decoy's effective function in suppressing the biological activity of STAT3 protein.

4 | DISCUSSION

Similar to the other malignancies, one of the most challenging clinical problems in treating colon cancer is drug resistance. Numerous studies have been conducted on resistance of cancer cells toward
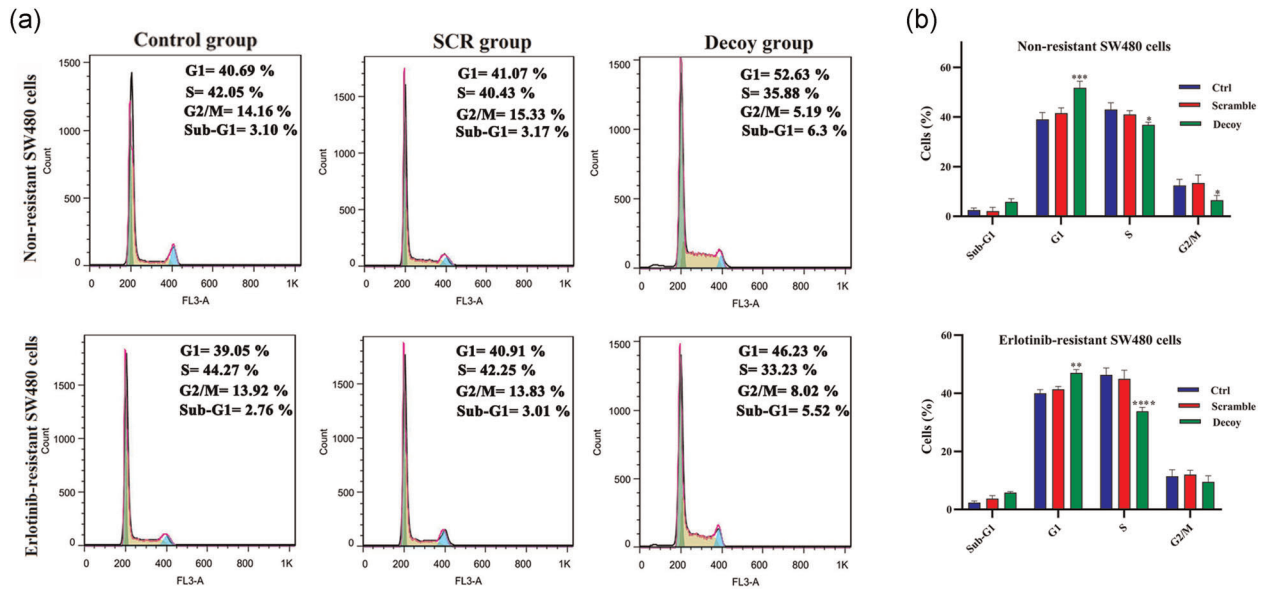
FIGURE 5 Analysis of ODNs (STAT3 decoy and scramble) effects on cell cycle profiles in both SW480 cell lines. (a) Treating nonresistant and resistant SW480 cells with 300 nM of STAT3 decoy caused G1 cell-cycle arrest as determined by the reduction in the cells in the S phase after 24 h. (b) The histogram illustrates the cell quantity of each phase of cell cycle in percent after treatment with decoy, scramble, and control. Two-way ANOVA was used as the statistical analysis. Values are assigned as mean ± SD in three independent experiments, *$p < .05$, **$p < .01$, ***$p < .001$, and ****$p < .0001$. ANOVA, analysis of variance; ODN, oligodeoxynucleotide; STAT3, signal transducer and activator of transcription 3

erlotinib, a common chemotherapy drug in colorectal cancer treatment (Fathi et al., 2013, 2015; Javadi et al., 2018). Previous studies have indicated a correlation between phosphorylated STAT3 (pSTAT3) and anti-EGFR–based therapy in colon cancer (Dobi et al., 2013; Ung et al., 2014; Zhuang et al., 2019). According to the earlier reports, an abnormal increase of STAT3 activation has demonstrated

to be connected with the elevated cell proliferation and invasion of colorectal cancer (H. Wang et al., 2020). As reported by Li et al., activation of STAT3/Bcl2/Bcl-XL survival pathway due to erlotinib treatment showed to be in association with cancer cell resistance toward erlotinib. However, erlotinib resistance was further reversed either through blocking of Tyr705 phosphorylation of STAT3 by
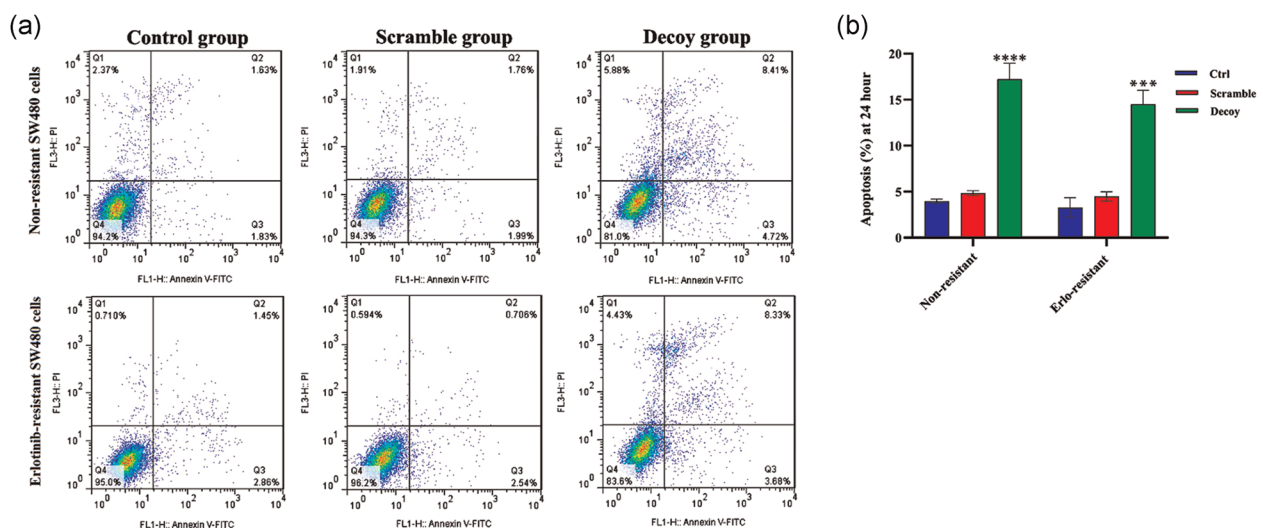

FIGURE 6 Apoptosis stimulated by STAT3 decoy ODNs in both nonresistant and resistant SW480 cell lines. (a) Flow cytometry analysis of nonresistant and resistant SW480 transfected cells with 300 nM ODNs (decoy and scramble) stained by annexin V/PI. (b) The histograms indicate the apoptotic cell percentages in the treated cells with STAT3 ODNs decoy, scramble, and control groups. Two-way ANOVA was used as the statistical analysis. Values are defined as the mean ± SD from three independent experiments, ***$p < .001$ and ****$p < .0001$. STAT3, signal transducer and activator of transcription 3; ODN, oligodeoxynucleotide; PI, propidium iodide

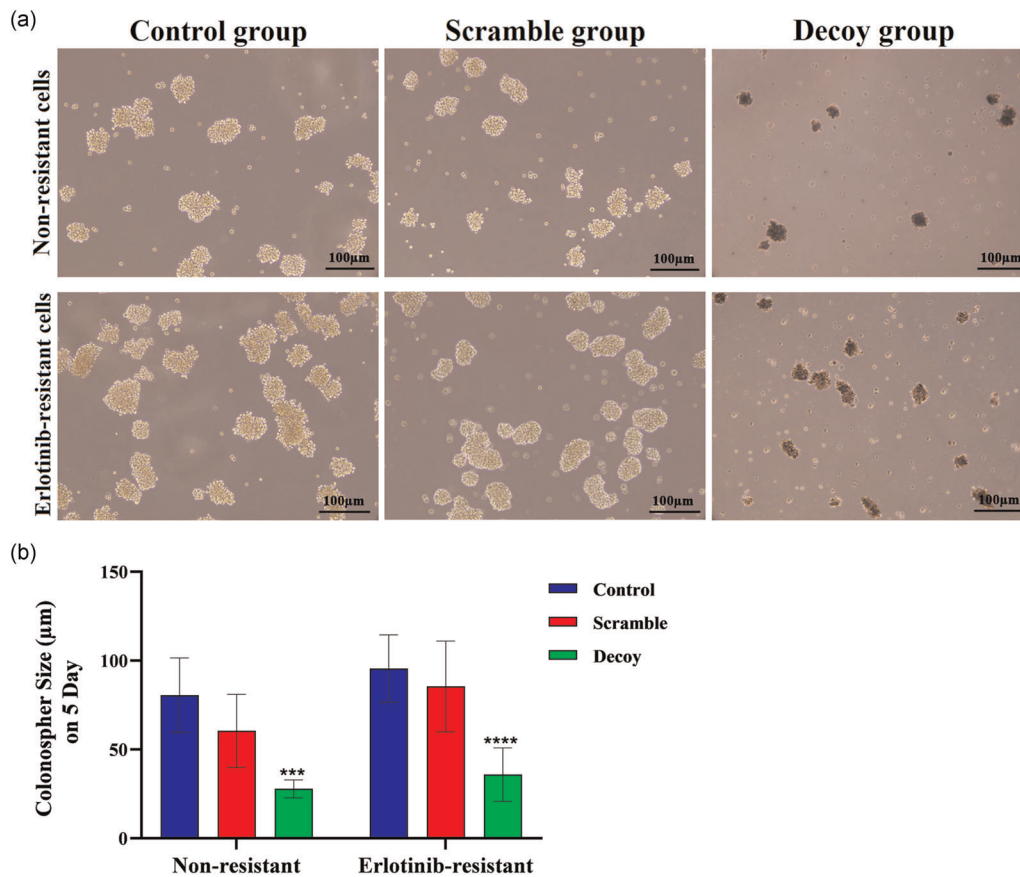**FIGURE 7** Colony formation assay of nonresistant and resistant SW480 cells following 5 days upon ODNs treatment. (a) Microscopic image of colony formation of SW480 cell lines treated with Lipofectamine as control, scramble, and decoy ODNs. (b) Statistical analysis of colonosphere size in the cell group treated with STAT3 decoy, compared with the scramble and control groups. Two-way ANOVA was used as the statistical analysis. The data are expressed as the mean ± SD of three independent experiments, ***$p < .001$ and ****$p < .0001$. ANOVA, analysis of variance; ODN, decoy oligodeoxynucleotide; STAT3, signal transducer and activator of transcription 3

niclosamide or STAT3 depletion due to RNA interference in HCC827/ER cells (Li et al., 2013).

The increasing prevalence of drug resistance in cancers necessitates the need to revolutionize the conventional treatments. The novel therapeutic candidate, known as transcription factor decoys, could neutralize key transcription factors by mimicking their consensus DNA binding sites. Recent researches have shed light on the fact that decoy ODNs can competitively hinder the binding of the related TF to the target sequences on promoters (Johari et al., 2019; Rahmati et al., 2020). In this study, the designed STAT3 decoy ODNs were evaluated as a potential tool to suppress the STAT3 signaling pathway by blocking the phosphorylated STAT3 and downregulation of STAT3 downstream oncogenes. In combination with anti-EGFR therapy, this method might restore the sensitivity to anticancer drugs in colon cancer cells.

Previously, it has been indicated that in silico analysis could be useful for optimizing the sequences of ODNs for blocking their target transcription factors (Bigdelou et al., 2019; Rahmati et al., 2020). In this study, first, the interactions of optimized ODNs with the DNA

binding site of STAT3 protein was investigated through molecular docking assay. The results of molecular docking revealed that binding of the decoy ODNs to the consensus site of the STAT3 protein is stronger in comparison with scrambled ODNs. It was indicated that Met331, Lys340, Gln344, Arg417, Arg423, Ser465, Asn466, Ile467, Cys468 residues of STAT3 protein were involved in the formation of H-bonds with decoy ODNs, while only Arg382, Arg414, Glu415, Arg417 residues interacted with scrambled ODNs. Differences in amino acids participating in decoy or scramble ODNs sequences interactions with the same target was demonstrating the influence of point mutations in identifying the DNA binding site at STAT3. The intact form of STAT3 protein (no mutation) was considered as the default in the study. The mutations have been designed in the sequence of oligodeoxynucleotides in the binding site of ODNs to the STAT3 protein. In silico analysis provided molecular and thermodynamic details of the interaction of ODNs to STAT3, where different numbers of H-bonds between decoy/STAT3 and scrambled/STAT3 resulted in higher stability of the folded state of decoy/STAT3 in terms of the energy profile.
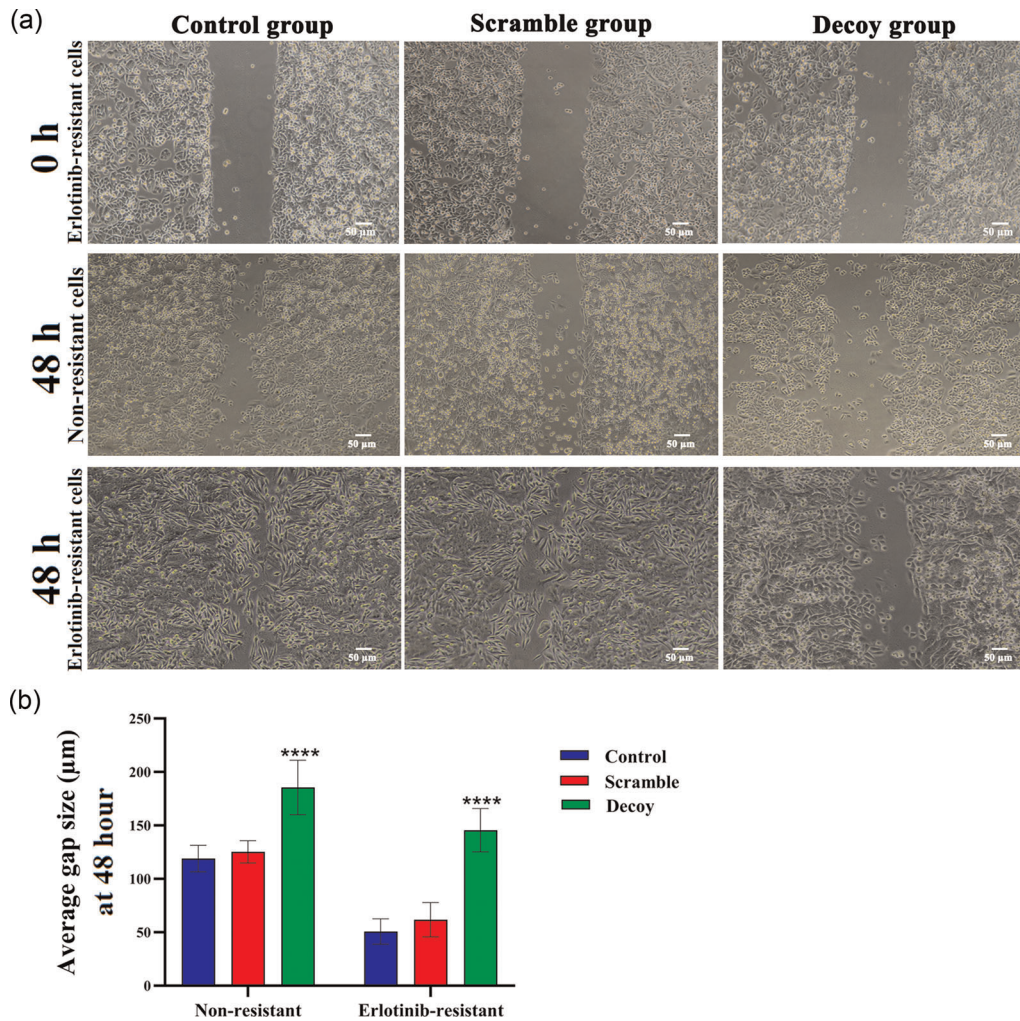
FIGURE 8 Cell migration capability was evaluated via scratch assay. (a) Following the linear scratching with a 10 µl sterile pipette tip, cells were treated with 300 nM ODNs. The process of scratch filling was followed for 48 h. (b) The mean gap size analysis indicated the significant slowing effect of STAT3 decoy treatment compared with the scramble and control groups. Two-way ANOVA was used as the statistical analysis. The data are expressed as the mean ± SD of three independent experiments, ****$p < .0001$. ANOVA, analysis of variance; ODN, oligodeoxynucleotide; STAT3, signal transducer and activator of transcription 3

The drug-resistant SW480 cell line was developed using a step-wise increase in the treatment dose of erlotinib. This induction of resistance caused approximately 160-fold higher resistance toward Erlotinib (IC50: 19/86 ± 1/8 µM) compared with the nonresistant cells (IC50: 124/2 ± 1/2 nM). Furthermore, the outcomes of MTT assay indicated that the inhibitory influences of STAT3 decoy ODNs on the cell viability of SW480 colon cancer cells decreases with a time-dependent pattern. In fact, the influences of STAT3 ODNs were time- and dose-dependent. The gradual declined inhibitory influences of STAT3 decoy ODNs might be due to its limited stability and ODNs concentration dilution during cell proliferation. ODNs might be degraded in a time-dependent manner by the nucleases which exist inside the cells.

Results of analyzing the cell cycle profile and apoptosis in STAT3 ODN-treated cells (nonresistant and resistant SW480 cells) were consistent with the results of inhibiting the STAT3 activity suppressed tumor cell proliferation by inducing cell cycle arrest and promotion of apoptosis (Wei et al., 2019). Ideally, equal seeding of the cells in each assay enable comparing the real effect of the treatment. However, the final results would be calculated based on the specific control of each cell line. The STAT3 decoy ODNs treatment resulted in cell cycle arrest at G0/G1 transition to the S phase, which was detected by elevating the number of cells in the G0/G1 phase and decreasing the number of cells in the S phase of both cell lines. In this regard, a distinctive increase in apoptotic cells was indicated in STAT3 decoy-treated cells to admit the inhibitory influence of decoy ODNs on STAT3 activity. Interestingly, a higher percentage of G0/G1 of non-resistant cells compared to the resistant cells in treatment with decoy might be due to a slight difference in the decrease of cyclin D1, as a regulator of G1-phase progression. Furthermore, subsequent to the lower percentage of resistant cells in S phase, there was a higher percentage of cells in G2/M in the treatment with the decoy that
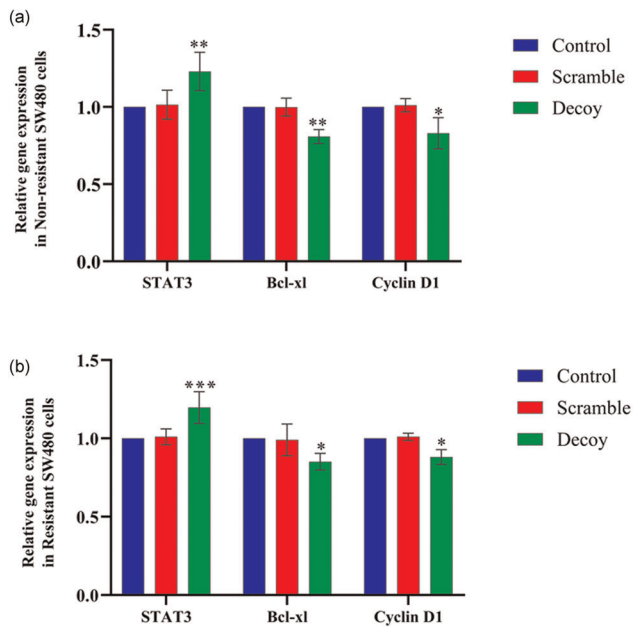
FIGURE 9 The effect of ODNs on the expression of STAT3 and its targeted genes involved in cell cycle and apoptosis regulation. After 24 h of transfection with 300 nM STAT3 decoy or scrambled ODNs, the extracted total RNA was used for cDNA synthesis and quantitative real-time PCR. The relative expression of genes was normalized to corresponding internal control in (a) nonresistant SW480 cells and (b) resistant SW480 cells. Two-way ANOVA was used as the statistical analysis. The data are expressed as the mean ± SD of three independent experiments, $^*p < .05$, $^{**}p < .01$, and $^{***}p < .001$ compared with the control group. ANOVA, analysis of variance; ODN, oligodeoxynucleotide; PCR, polymerase chain reaction; STAT3, signal transducer and activator of transcription 3

could be interpreted as the higher transition of the resistant cells into G2/M. The strong effect of STAT3 ODNs on the nonresistant cells compared with the resistant ones could be due to the high proliferation and high activity of STAT3 transcription factor in resistant cells, implying that STAT3 might be employed as a potential target for gene therapy in CRC patients.

The binding of STAT3-decoy ODNs with STAT3 transcription factor was expected to induce the cytoplasmic entanglement of STAT3, and blocking the nuclear transfer of activated STAT3. Accordingly, the influence of STAT3 decoy ODNs on the expression of downstream genes was determined. Relative expression analysis indicated downregulation of antiapoptotic *Bcl-xl* gene and cell cycle regulatory gene (*cyclin D1*), due to the suppression of STAT3 after decoy treatment. Moreover, detecting the upregulation of the STAT3 gene in nonresistant and resistant decoy-treated cells could be interpreted as a relatively compensatory effort (as negative feedback) of STAT3 inhibition compared with control and scramble groups. The cell cycle arrest in G0/G1 and promoted cell apoptosis, revealed that STAT3 decoy ODNs could competitively inhibit the binding of activated STAT3 transcription factor and endogenous cis-elements in its downstream target genes.

In agreement with the compelling evidence that reported deletion of STAT3 disrupted cell migration (Kulesza et al., 2019; Y. Wang

et al., 2017), the influences of STAT3 decoy ODN treatment on the migration potential of cells were observed in a scratch assay. In the other words, wound healing occurred slower in decoy-treated cells compared with control groups. This result could confirm that designed decoy ODNs were able to inhibit STAT3 function (Johari et al., 2020).

As expected, colony formation was influenced by STAT3 inhibition, too (Callejas et al., 2019). A significant decrease in colony size of both nonresistant and resistant SW480 cells was observed in treatment with STAT3 decoy ODN, as opposed to treatment with scrambled ODNs and control.

Altogether, the results from different assays performed in our study demonstrated that the influence of the decoy ODNs were the highest at 300 nM in the nonresistant cells than the erlotinib-resistant ones, which could be due to the high expression level and activity of the STAT3 protein, and the higher phosphorylation of this transcription factor in the resistant cells.

In a previous study, we established the SW480 resistant toward the erlotinib and investigated the levels of integrin αvβ3 in these resistant cells. The obtained results showed that the expression of integrin was elevated in the resistant cells (Javadi et al., 2018). Previously, it has been indicated that the upregulation of integrins is a common property of erlotinib-resistant NSCLC cell lines and erlotinib-refractory tumor samples (Kanda et al., 2013; Seguin et al., 2014). Activation of the αvβ3–KRAS–RalB–NF-κB as a bypass effector pathway has been suggested as a main factor and necessary for resistance toward erlotinib. KRAS could activate the downstream RalB/NFκB pathway which causes therapy resistance by enhancing a stem cell-like phenotype (Seguin et al., 2014). In SW480 cells, both NF-κB and STAT3 are triggered, which suggests a constitutive interleukin secretory loop, since it has been demonstrated for several tumor cell systems (Bollrath & Greten, 2009). Souissi et al. (2011) have demonstrated that active STAT3 interacts with NF-κB in the colon-carcinoma SW480 cells, as indicated by the presence of NF-κB in STAT3-decoy ODN pull-downs and by decreased NF-κB transcriptional activity. Therefore, by trapping active STAT3 inside the cytoplasm, STAT3-decoy ODN could simultaneously arrest the fraction of NF-κB that is connected with active STAT3. This mechanism could potentially permit the targeting of a subset of genes that are necessary for uncontrolled tumor cell growth and drug resistance. Genetically or pharmacological targeting this pathway has shown to be capable of reversing the cancer stemness and drug resistance (Figure 10).

Considering the benefits of TFD over the other STAT3 inhibitor strategies, such as small interfering RNA and monoclonal antibodies, specificity and efficiency in target binding, alongside the lower expenses of decoy ODNs synthesis, provides interest to the researchers (An et al., 2020; Gwon et al., 2020). Despite limitations in clinical development of ODNs in terms of stability and effective cell transfer, structural modifications are proposed to overcome these barriers and introduce ODNs as therapeutic candidates, especially in cases of drug resistance (Hecker & Wagner, 2017; Rao et al., 2020). These advantages have made the clinical application of STAT3
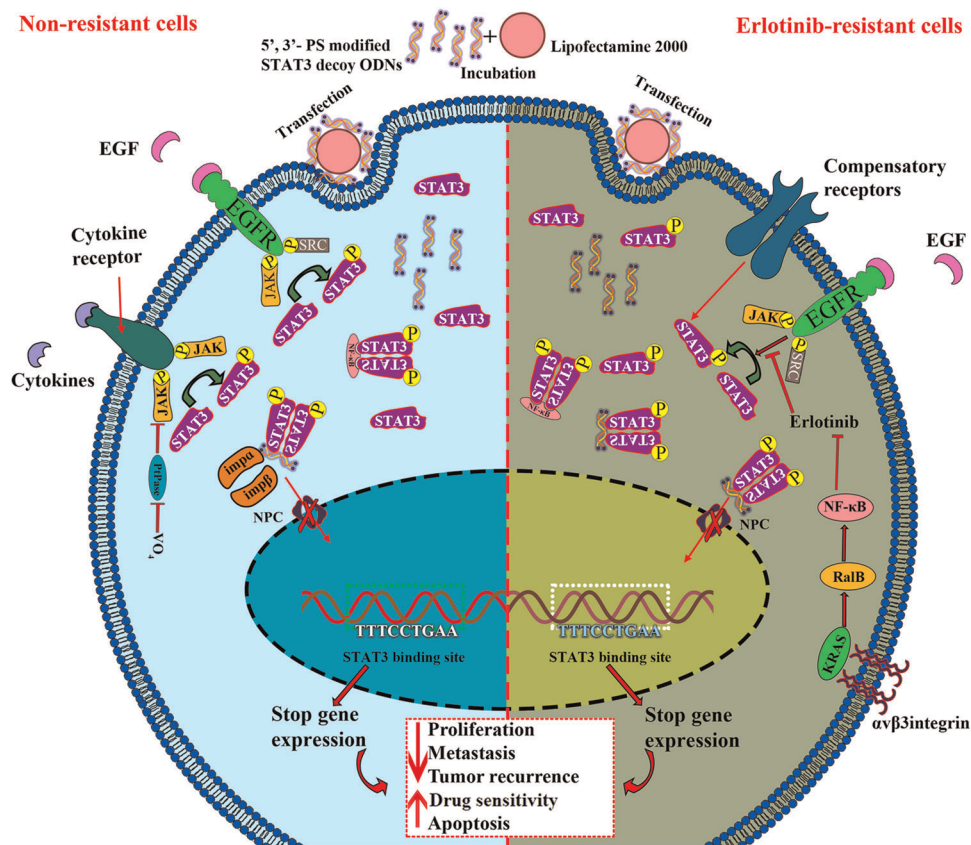
FIGURE 10 Overview of suppressing the metastatic properties in both nonresistant and erlotinib-resistant colon cancer cells using a STAT3 decoy ODNs. EGF, epidermal growth factor; EGFR, epidermal growth factor receptor; JAK, janus kinase; NF-κB, nuclear factor-κB; NPC, nasopharyngeal carcinoma; ODN, oligodeoxynucleotide; STAT3, signal transducer and activator of transcription 3

possible, for example, a report by Sen et al. (2012b) who registered the first clinical trial of STAT3 decoy ODNs in head and neck tumors. Altogether, TFD approach by using refined and optimized decoy ODNs is about to be a tangible therapeutic option for STAT3 inhibition, beyond other targets for disease treatment (Bigdelou et al., 2020; Uchida et al., 2020).

5 | CONCLUSION

This study demonstrated promising results for inhibiting metastatic properties related to STAT3 function by using the designed decoy ODNs in both nonresistant and erlotinib-resistant SW480 cells. The effect of STAT3 decoy ODNs on resistant colon cancer cells indicated to be effective for suppressing the STAT3 signaling in drug-resistant colon cancer cells. Future studies, such as investigating the synergistic effect of anti-EGFR agents with STAT3 decoy ODNs are required to provide more effective treatments for CRC patients.

CONFLICT OF INTERESTS

The authors declare that there are no conflict of interests.

AUTHOR CONTRIBUTIONS

Conceptualization and study design: Behrooz Johari. *Data collection, assembly, and writing the original draft*: Zoleykha Asadi, Behrooz Johari, Elham Rismani, and Zahra Bigdelou. *Final approval of the final draft*: Mojtaba Fathi and Behrooz Johari.

DATA AVAILABILITY STATEMENT

The data sets used and/or analyzed during the current study are available from the corresponding author on reasonable request.

ORCID

Behrooz Johari http://orcid.org/0000-0003-3440-572X

REFERENCES

An, H.-J., Kim, J.-Y., Gwon, M.-G., Gu, H., Kim, H.-J., Leem, J., Youn, S. W., & Park, K. K. (2020). Beneficial Effects of SREBP Decoy Oligodeoxynucleotide in an Animal Model of Hyperlipidemia. *International Journal of Molecular Sciences, 21*, 552.

Becker, S., Groner, B., & Muller, C. W. (1998). Three-dimensional structure of the Stat3beta homodimer bound to DNA. *Nature, 394*, 145–151.

Bigdelou, Z., Johari, B., Kadivar, M., Rismani, E., Asadi, Z., Rahmati, M., & Saltanatpour, Z. (2019). Investigation of specific binding of designed oligodeoxynucleotide decoys to transcription factors in HT29 cell line undergoing epithelial–mesenchymal transition (EMT). *Journal of Cellular Physiology, 234*, 22765–22774.

Bigdelou, Z., Mortazavi, Y., Saltanatpour, Z., Asadi, Z., Kadivar, M., & Johari, B. (2020). Role of Oct4–Sox2 complex decoy oligodeoxynucleotides strategy on reverse epithelial to mesenchymal transition (EMT) induction in HT29-ShE encompassing enriched cancer stem-like cells. *Molecular Biology Reports, 47*, 1859-1869.

Bollrath, J., & Greten, F. R. (2009). IKK/NF-κB and STAT3 pathways: Central signalling hubs in inflammation-mediated tumour promotion and metastasis. *EMBO Reports, 10*, 1314–1319.

Callejas, B. E., Mendoza-Rodríguez, M. G., Villamar-Cruz, O., Reyes-Martínez, S., Sánchez-Barrera, C. A., Rodríguez-Sosa, M., Delgado-Buenrostro, N. L., Martínez-Saucedo, D., Chirino, Y. I., León-Cabrera, S. A., Pérez-Plasencia, C., Vaca-Paniagua, F., Arias-Romero, L. E., & Terrazas, L. I. (2019). Helminth-derived molecules inhibit colitis-associated colon cancer development through NF-κB and STAT3 regulation. *International Journal of Cancer, 145*, 3126–3139.

Chen, A. M., Zhang, M., Wei, D., Stueber, D., Taratula, O., Minko, T., & He, H. (2009). Co-delivery of doxorubicin and Bcl-2 siRNA by mesoporous silica nanoparticles enhances the efficacy of chemotherapy in multidrug-resistant cancer cells. *Small, 5*, 2673–2677.

van Dijk, M., & Bonvin, A. M. J. J. (2009). 3D-DART: A DNA structure modelling server. *Nucleic Acids Research, 37*, W235–W9.

Dobi, E., Monnien, F., Kim, S., Ivanaj, A., N'Guyen, T., Demarchi, M., Adotevi, O., Thierry-Vuillemin, A., Jary, M., Kantelip, B., Pivot, X., Godet, Y., Degano, S. V., & Borg, C. (2013). Impact of STAT3 phosphorylation on the clinical effectiveness of anti-EGFR–based therapy in patients with metastatic colorectal cancer. *Clinical Colorectal Cancer, 12*, 28–36.

Fathi, M., Taghikhani, M., Ghannadi-Maragheh, M., & Yavari, K. (2013). Demonstration of dose dependent cytotoxic activity in SW480 colon cancer cells by 177Lu-labeled siRNA targeting IGF-1R. *Nuclear Medicine and Biology, 40*, 529–536.

Fathi, M., Yavari, K., Taghikhani, M., & Ghannadi Maragheh, M. (2015). Synthesis of a stabilized 177Lu–siRNA complex and evaluation of its stability and RNAi activity. *Nuclear Medicine Communications, 36*, 636–645.

Gharibi, T., Babaloo, Z., Hosseini, A., Abdollahpour-Alitappeh, M., Hashemi, V., Marofi, F., Nejati, K., & Baradaran, B. (2020). Targeting STAT3 in cancer and autoimmune diseases. *European Journal of Pharmacology, 878*, 173107.

Gu, J., Li, G., Sun, T., Su, Y., Zhang, X., Shen, J., Tian, Z., & Zhang, J. (2008). Blockage of the STAT3 signaling pathway with a decoy oligonucleotide suppresses growth of human malignant glioma cells. *Journal of Neuro-Oncology, 89*, 9–17.

Gwon, M. G., An, H. J., Kim, J. Y., Kim, W. H., Gu, H., Kim, H. J., Leem, J., Jung, H. J., & Park, K. K. (2020). Anti-fibrotic effects of synthetic TGF-β1 and Smad oligodeoxynucleotide on kidney fibrosis in vivo and in vitro through inhibition of both epithelial dedifferentiation and endothelial-mesenchymal transitions. *The FASEB Journal, 34*, 333–349.

Haghighi, O., & Moradi, M. (2020). In Silico Study of the Structure and Ligand Interactions of Alcohol Dehydrogenase from Cyanobacterium Synechocystis Sp. PCC 6803 as a Key Enzyme for Biofuel Production. *Applied Biochemistry and Biotechnology, 192*, 1–22.

Hajighasemlou, S., Alebouyeh, M., Rastegar, H., Manzari, M, T., Mirmoghtadaei, M., Moayedi, B., Ahmadzadeh, M., Parvizpour, F., Johari, B., Naeini, M, M., & Farajollahi, M. M. (2015). Preparation of immunotoxin herceptin-botulinum and killing effects on two breast cancer cell lines. *Asian Pacific journal of cancer prevention, 16*, 5977–5981.

Hecker, M., & Wagner, A. H. (2017). Transcription factor decoy technology: A therapeutic update. *Biochemical Pharmacology, 144*, 29–34.

Hu, C.-M. J., & Zhang, L. (2012). Nanoparticle-based combination therapy toward overcoming drug resistance in cancer. *Biochemical Pharmacology, 83*, 1104–1111.

Javadi, S., Rostamizadeh, K., Hejazi, J., Parsa, M., & Fathi, M. (2018). Curcumin mediated down-regulation of αVβ3 integrin and up-regulation of pyruvate dehydrogenase kinase 4 (PDK4) in Erlotinib resistant SW480 colon cancer cells. *Phytotherapy Research, 32*, 355–364.

Johari, B., Asadi, Z., Rismani, E., Maghsood, F., Sheikh Rezaei, Z., Farahani, S., Madanchi, H., & Kadivar, M. (2019). Inhibition of transcription factor T-cell factor 3 (TCF3) using the oligodeoxynucleotide strategy increases embryonic stem cell stemness: Possible application in regenerative medicine. *Cell Biology International, 43*, 852–862.

Johari, B., Rahmati, M., Nasehi, L., Mortazavi, Y., Faghfoori, M. H., & Rezaeejam, H. (2020). Evaluation of STAT3 decoy oligodeoxynucleotides' synergistic effects on radiation and/or chemotherapy in metastatic breast cancer cell line. *Cell Biology International, 44*, 2499–2511.

Kanda, R., Kawahara, A., Watari, K., Murakami, Y., Sonoda, K., Maeda, M., Fujita, H., Kage, M., Uramoto, H., Costa, C., Kuwano, M., & Ono, M. (2013). Erlotinib resistance in lung cancer cells mediated by integrin β1/Src/Akt-driven bypass signaling. *Cancer Research, 73*, 6243–6253.

Kulesza, D. W., Ramji, K., Maleszewska, M., Mieczkowski, J., Dabrowski, M., Chouaib, S., & Kaminska, B. (2019). Search for novel STAT3-dependent genes reveals SERPINA3 as a new STAT3 target that regulates invasion of human melanoma cells. *Laboratory Investigation, 99*, 1607–1621.

Lasala, G. P., & Minguell, J. J. (2011). Vascular disease and stem cell therapies. *British Medical Bulletin, 98*, 98–197.

Laskowski, R. A., & Swindells, M. B. (2011). LigPlot+: Multiple Ligand–Protein Interaction Diagrams for Drug Discovery. *Journal of Chemical Information and Modeling, 51*, 2778–2786.

Li, R., Hu, Z., Sun, S.-Y., Chen, Z. G., Owonikoko, T. K., Sica, G. L., Ramalingam, S. S., Curran, W. J., Khuri, F. R., & Deng, X. (2013). Niclosamide overcomes acquired resistance to erlotinib through suppression of STAT3 in non–small cell lung cancer. *Molecular Cancer Therapeutics, 12*, 2200–2212.

Liu, S., Dontu, G., Mantle, I. D., Patel, S., Ahn, N., Jackson, K. W., Suri, P., & Wicha, M. S. (2006). Hedgehog signaling and Bmi-1 regulate self-renewal of normal and malignant human mammary stem cells. *Cancer Research, 66*, 6063–6071.

Nabati, F., Moradi, M., & Mohabatkar, H. (2020). In silico analyzing the molecular interactions of plant-derived inhibitors against E6AP, p53, and c-Myc binding sites of HPV type 16 E6 oncoprotein. *Molecular Biology Research Communications, 9*, 71–82.

Phi, L. T. H., Wijaya, Y. T., Sari, I. N., Yang, Y. G., Lee, Y. K., & Kwon, H. Y. (2018). The anti-metastatic effect of ginsenoside Rb2 in colorectal cancer in an EGFR/SOX2-dependent manner. *Cancer Medicine, 7*, 5621–5631.

Preston, S., Alison, M., Forbes, S., Direkze, N., Poulsom, R., & Wright, N. (2003). The new stem cell biology: Something for everyone. *Molecular Pathology, 56*, 86–96.

Rahmati, M., Johari, B., Kadivar, M., Rismani, E., & Mortazavi, Y. (2020). Suppressing the metastatic properties of the breast cancer cells using STAT3 decoy oligodeoxynucleotides: A promising approach for eradication of cancer cells by differentiation therapy. *Journal of Cellular Physiology, 235*, 5429–5444.

Rao, C., Ni, Y. R., Zhao, Y. M., Zhang, Y. Q., Zhou, R. T., Liu, C. B., Han, L., Wu, J.-F. (2020). Class C1 decoy oligodeoxynucleotide inhibits profibrotic genes expression in rat hepatic stellate cells. *Molecular Medicine Reports, 21*, 667–674.

Roberts, C. M., Shahin, S. A., Wen, W., Finlay, J. B., Dong, J., Wang, R., Dellinger, T. H., Zink, J. I., Tamanoi, F., & Glackin, C. A. (2017).

Nanoparticle delivery of siRNA against TWIST to reduce drug resistance and tumor growth in ovarian cancer models. *Nanomedicine: Nanotechnology, Biology and Medicine, 13,* 965–976.

Seguin, L., Kato, S., Franovic, A., Camargo, M. F., Lesperance, J., Elliott, K. C., Yebra, M., Mielgo, A., Lowy, A. M., Husain, H., Cascone, T., Diao, L., Wang, J., Wistuba, I. I., Heymach, J. V., Lippman, S. M., Desgrosellier, J. S., Anand, S., Weis, S. M., & Cheresh, D. A. (2014). An integrin β 3–KRAS–RalB complex drives tumour stemness and resistance to EGFR inhibition. *Nature Cell Biology, 16,* 457–468.

Sen, M., Joyce, S., Panahandeh, M., Li, C., Thomas, S. M., Maxwell, J., Wang, L., Gooding, W. E., Johnson, D. E., & Grandis, J. R. (2012a). Targeting Stat3 abrogates EGFR inhibitor resistance in cancer. *Clinical Cancer Research, 18,* 4986–4996.

Sen, M., Thomas, S. M., Kim, S., Yeh, J. I., Ferris, R. L., Johnson, J. T., Duvvuri, U., Lee, J., Sahu, N., Joyce, S., Freilino, M. L., Shi, H., Li, C., Ly, D., Rapireddy, S., Etter, J. P., Li, P. K., Wang, L., Chiosea, S., ... Grandis, J. R. (2012b). First-in-human trial of a STAT3 decoy oligonucleotide in head and neck tumors: Implications for cancer therapy. *Cancer Discovery, 2,* 694–705.

Snir, M., Kehat, I., Gepstein, A., Coleman, R., Itskovitz-Eldor, J., Livne, E., & Gepstein, L. (2003). Assessment of the ultrastructural and proliferative properties of human embryonic stem cell-derived cardiomyocytes. *American Journal of Physiology-Heart and Circulatory Physiology, 285,* H2355–H2363.

Souissi, I., Najjar, I., Ah-Koon, L., Schischmanoff, P., Lesage, D., Le Coquil, S., Roger, C., Dusanter-Fourt, I., Varin-Blank, N., Cao, A., Metelev, V., Baran-Marszak, F., & Fagard, R. (2011). A STAT3-decoy oligonucleotide induces cell death in a human colorectal carcinoma cell line by blocking nuclear transfer of STAT3 and STAT3-bound NF-κB. *BMC Cell Biology, 12,* 1–19.

Szakács, G., Paterson, J. K., Ludwig, J. A., Booth-Genthe, C., & Gottesman, M. M. (2006). Targeting multidrug resistance in cancer. *Nature Reviews Drug Discovery, 5,* 219–234.

Tadlaoui Hbibi, A., Laguillier, C., Souissi, I., Lesage, D., Le Coquil, S., Cao, A., Metelev, V., Baran-Marszak, F., & Fagard, R. (2009). Efficient killing of SW480 colon carcinoma cells by a signal transducer and activator of transcription (STAT) 3 hairpin decoy oligodeoxynucleotide–interference with interferon-γ-STAT1-mediated killing. *The FEBS Journal, 276,* 2505–2515.

Tong, J., Tan, S., Zou, F., Yu, J., & Zhang, L. (2017). FBW7 mutations mediate resistance of colorectal cancer to targeted therapies by blocking Mcl-1 degradation. *Oncogene, 36,* 787–796.

Triner, D., Castillo, C., Hakim, J. B., Xue, X., Greenson, J. K., Nuñez, G., Chen, G. Y., Colacino, J. A., & Shah, Y. M. (2018). Myc-associated zinc finger protein regulates the Proinflammatory response in colitis and Colon Cancer via STAT3 signaling. *Molecular and Cellular Biology, 38,* 38.

Troiani, T., Napolitano, S., Vitagliano, D., Morgillo, F., Capasso, A., Sforza, V., Nappi, A., Ciardiello, D., Ciardiello, F., & Martinelli, E. (2014). Primary and acquired resistance of colorectal cancer cells to anti-EGFR antibodies converge on MEK/ERK pathway activation and can be overcome by combined MEK/EGFR inhibition. *Clinical Cancer Research, 20,* 3775–3786.

Uchida, D., Saito, Y., Kikuchi, S., Yoshida, Y., Hirata, S., Sasajima, T., & Azuma, N. (2020). Development of gene therapy with a cyclic adenosine monophosphate response element decoy oligodeoxynucleotide to prevent vascular intimal hyperplasia. *Journal of Vascular Surgery, 71,* 229–241.

Ung, N., Putoczki, T. L., Stylli, S. S., Ng, I., Mariadason, J. M., Chan, T. A., Zhu, H. J., & Luwor, R. B. (2014). Anti-EGFR therapeutic efficacy correlates directly with inhibition of STAT3 activity. *Cancer Biology & Therapy, 15,* 623–632.

Wang, H., Liu, Z., Guan, L., Li, J., Chen, S., Yu, W., & Lai, M. (2020). LYW-6, a Novel Cryptotanshinone Derived STAT3 Targeting Inhibitor, Suppresses Colorectal Cancer Growth and Metastasis. *Pharmacological Research, 153,* 104661.

Wang, Y., Lu, Z., Wang, N., Zhang, M., Zeng, X., & Zhao, W. (2017). MicroRNA-1299 is a negative regulator of STAT3 in colon cancer. *Oncology Reports, 37,* 3227–3234.

Wassenaar, T. A., van Dijk, M., Loureiro-Ferreira, N., van der Schot, G., de Vries, S. J., Schmitz, C., van der Zwan, J., Boelens, R., Giachetti, A., Ferella, L., Rosato, A., Bertini, I., Herrmann, T., Jonker, H. R. A., Bagaria, A., Jaravine, V., Güntert, P., Schwalbe, H., Vranken, W. F., ... Bonvin, A. M. J. J. (2012). WeNMR: Structural Biology on the Grid. *Journal of Grid Computing, 10,* 743–767.

Wei, N., Li, J., Fang, C., Chang, J., Xirou, V., Syrigos, N. K., Marks, B. J., Chu, E., & Schmitz, J. C. (2019). Targeting colon cancer with the novel STAT3 inhibitor bruceantinol. *Oncogene, 38,* 1676–1687.

Weickhardt, A. J., Price, T. J., Chong, G., Gebski, V., Pavlakis, N., Johns, T. G., Azad, A., Skrinos, E., Fluck, K., Dobrovic, A., Salemi, R., Scott, A. M., Mariadason, J. M., & Tebbutt, N. C. (2012). Dual targeting of the epidermal growth factor receptor using the combination of cetuximab and erlotinib: Preclinical evaluation and results of the phase II DUX study in chemotherapy-refractory, advanced colorectal cancer. *Journal of Clinical Oncology, 30,* 1505–1512.

Zhuang, Y., Bai, Y., Hu, Y., Guo, Y., Xu, L., Hu, W., Yang, L., Zhao, C., Li, X., & Zhao, H. (2019). Rhein sensitizes human colorectal cancer cells to EGFR inhibitors by inhibiting STAT3 pathway. *OncoTargets and Therapy, 12,* 5281–5291.

van Zundert, G. C. P., Rodrigues, J. P. G. L. M., Trellet, M., Schmitz, C., Kastritis, P. L., Karaca, E., Melquiond, A. S. J., van Dijk, M., de Vries, S. J., & Bonvin, A. M. J. J. (2016). The HADDOCK2.2 Web Server: User-Friendly Integrative Modeling of Biomolecular Complexes. *Journal of Molecular Biology, 428,* 720–725.

SUPPORTING INFORMATION

Additional Supporting Information may be found online in the supporting information tab for this article.